DOI: 10.1002/asia.200600082

Structure-Dependent Photoinduced Electron Transfer in Fullerodendrimers with Light-Harvesting Oligophenylenevinylene Terminals

Nicola Armaroli,*[a] Gianluca Accorsi,[a] John N. Clifford,[a] Jean-François Eckert,[b] and Jean-François Nierengarten*[b]

Abstract: Oligophenylenevinylene (OPV)-terminated phenylenevinylene dendrons **G1**–**G4** with one, two, four, and eight "side-arms", respectively, were prepared and attached to C_{60} by a 1,3-dipolar cycloaddition of azomethine ylides generated in situ from dendritic aldehydes and *N*-methylglycine. The relative electronic absorption of the OPV moiety increases progressively along the fullerodendrimer family **C_{60}G1**–**C_{60}G4**, reaching a 99:1 ratio for **C_{60}G4** (antenna effect). UV/Vis and near-IR luminescence and transient absorption spectroscopy was used to elucidate photoinduced energy and electron transfer in **C_{60}G1**–**C_{60}G4** as a function of OPV moiety size and solvent polarity (toluene, dichloromethane, benzonitrile), taking into account the fact that the free-energy change for electron transfer is the same along the series owing to the invariability of the donor–acceptor couple. Regardless of solvent, all the fullerodendrimers exhibit ultrafast OPV→C_{60} singlet energy transfer. In CH_2Cl_2, the OPV→C_{60} electron transfer from the lowest fullerene singlet level ($^1C_{60}$*) is slightly exergonic ($\Delta G_{CS} \approx 0.07$ eV), but is observed, to an increasing extent, only in the largest systems **C_{60}G2**–**C_{60}G4** with lower activation barriers for electron transfer. This effect has been related to a decrease of the reorganization energy upon enlargement of the molecular architecture. Structural factors are also at the origin of an unprecedented OPV→C_{60} electron transfer observed for **C_{60}G3** and **C_{60}G4** in apolar toluene, whereas in benzonitrile, electron transfer occurs in all cases. Monitoring of the lowest fullerene triplet state by sensitized singlet oxygen luminescence and transient absorption spectroscopy shows that this level is populated through intersystem crossing and is not involved in photoinduced electron transfer.

Keywords: dendrimers · electron transfer · energy transfer · fullerenes · luminescence · singlet oxygen

Introduction

Due to their unique branched structure, dendrimers are intrinsically original scaffolds for the preparation of photoactive molecular devices,[1–9] and a particularly appealing feature is based on the possibility of producing multichromophoric ensembles that mimic the characteristic features of the natural photosynthetic system.[10,11] In such dendrimer-based photoactive devices, an array of peripheral chromophores is able to transfer the collected energy to the central core of the dendrimer, thus mimicking the natural light-harvesting complex where antenna molecules collect sunlight and channel the absorbed energy to a single reaction center. Furthermore, in the most-sophisticated systems, this initial transduction of excitation energy can be followed by an electron-transfer event as observed in natural photosynthetic systems.[10,11] These studies are not only important for the fundamental understanding of photoinduced processes, but appear to be of great interest for the design of new photovoltaic materials with optimized absorption properties[12,13] or for the preparation of efficient light-emitting devices.[14]

[60]Fullerene (C_{60}) is an attractive functional core for the preparation of such light-harvesting dendrimers.[15] Effectively, its lowest singlet and triplet excited states are rela-

[a] Dr. N. Armaroli, Dr. G. Accorsi, Dr. J. N. Clifford
Molecular Photoscience Group
Istituto per la Sintesi Organica e la Fotoreattività del CNR
Via Gobetti 101, 40129 Bologna (Italy)
Fax: (+39) 051-639-9844
E-mail: armaroli@isof.cnr.it

[b] Dr. J.-F. Eckert, Dr. J.-F. Nierengarten
Groupe de Chimie des Fullerènes et des Systèmes Conjugués
Laboratoire de Chimie de Coordination du CNRS
205 route de Narbonne, 31077 Toulouse Cedex 4 (France)
Fax: (+33) 561-553-003
E-mail: jfnierengarten@lcc-toulouse.fr

Supporting information for this article is available on the WWW under http://www.chemasianj.org or from the author.

tively low in energy, and photoinduced energy-transfer events have been observed in numerous fullerene-based dyads.[16] Furthermore, C_{60} is a good electron acceptor in photochemical molecular devices. Several examples of dendrimers with a fullerene core and phenylenevinylene[17–20] or phenyleneethynylene[21,22] dendritic branches have been reported so far. Remarkable light-harvesting capability of the peripheral units relative to the central core has been observed in these compounds. Martin, Guldi, and co-workers have shown that the end-capping of the dendritic phenylenevinylene spacer with dibutylaniline units yields a multicomponent photoactive system in which the dendritic wedge plays simultaneously the role of an antenna capable of channeling the absorbed energy to the fullerene core and of an electron-donating unit.[18] Photophysical investigations in benzonitrile solutions have shown that, upon photoexcitation, efficient and fast energy transfer takes place from the initially excited antenna moiety to the fullerene core. This process populates the lowest fullerene singlet excited state that is able to promote electron transfer from the dendritic unit to the fullerene core. Langa et al. have also prepared related fullerodendrimers in which the phenylenevinylene dendritic wedge is connected to a pyrazolino[60]fullerene core. Preliminary photophysical investigations suggest that the efficient energy transfer from the excited antenna moiety to the pyrazolino[60]fullerene core is followed by an electron transfer involving the fullerene moiety and the pyrazoline N atom.[20] As part of this research, we have prepared dendrimers **C_{60}G1**–**C_{60}G3**, and preliminary photophysical investigations have revealed that these compounds are interesting systems with light-harvesting properties.[17] Herein, we describe the preparation of the next-generation derivative **C_{60}G4** and report in detail on the photophysical properties of the whole series of compounds. Light-harvesting oligophenylenevinylene (OPV) moieties convey excitation energy to the carbon sphere by singlet energy transfer. The singlet fullerene excited state thus generated triggers an electron-transfer process that is dramatically dependent on medium polarity and dendrimer structure.

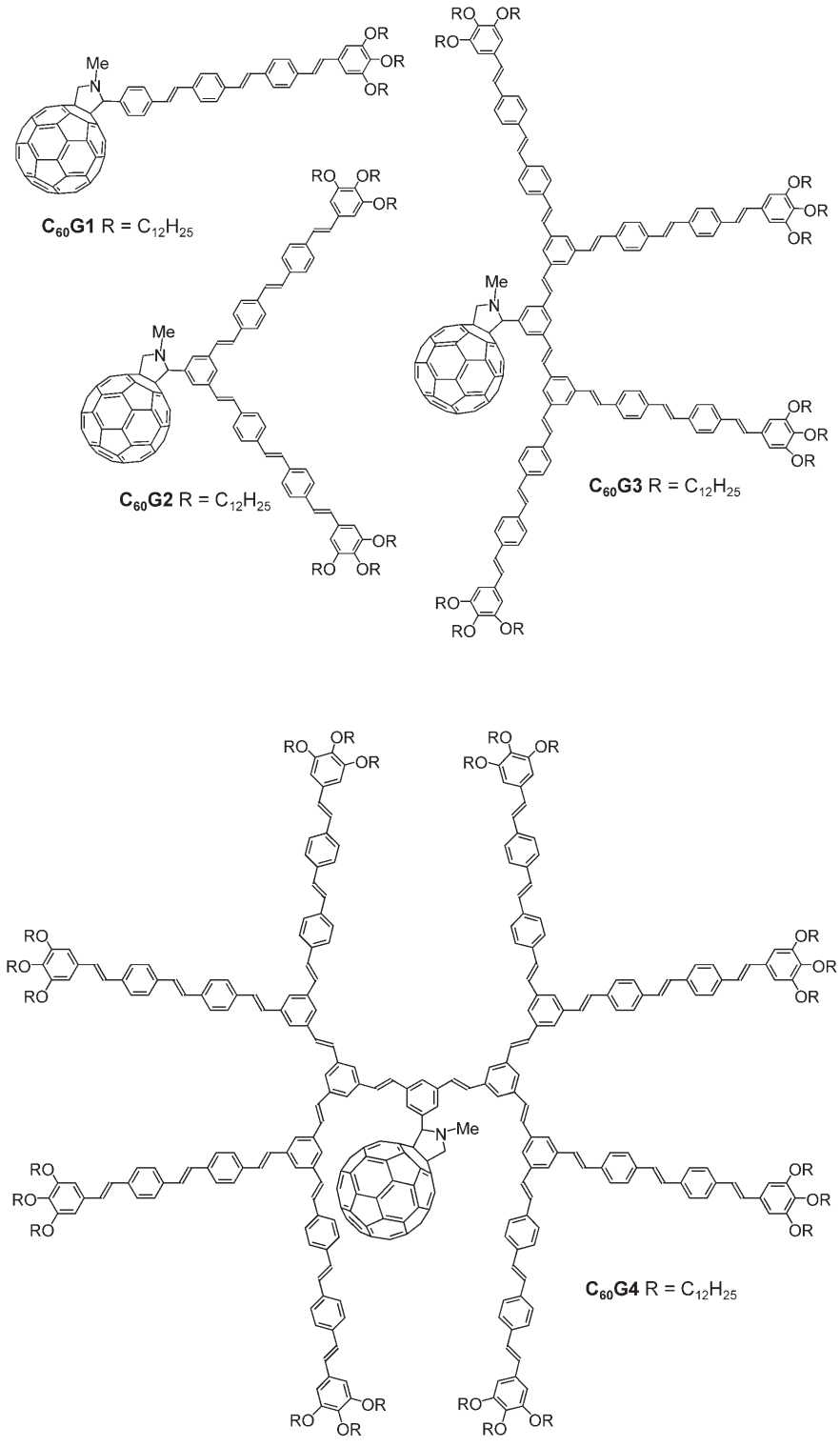

Results and discussion

Synthesis

The preparation of C_{60}**G1** is depicted in Scheme 1. Compound **1** was obtained in two steps from *p*-bromobenzaldehyde as previously reported.[23] Reduction with $LiAlH_4$ followed by bromination of the resulting alcohol **2** with CBr_4/PPh_3 gave **3**. Subsequent treatment with $P(OEt)_3$ then afforded phosphonate **4**. Reaction of **4** with aldehyde **5** under Wadsworth–Emmons conditions yielded the OPV tetramer **6**, which after treatment with CF_3CO_2H gave **7**. The functionalization of C_{60} was based on the 1,3-dipolar cycloaddition of the azomethine ylide[24] generated in situ from **7**. The reaction of C_{60} with **7** in the presence of an excess of *N*-methylglycine in refluxing toluene gave C_{60}**G1** in 46% yield. Compound **G1**, which was used as a reference compound for absorption and emission properties, was also prepared by reduction of **7** with $LiAlH_4$.

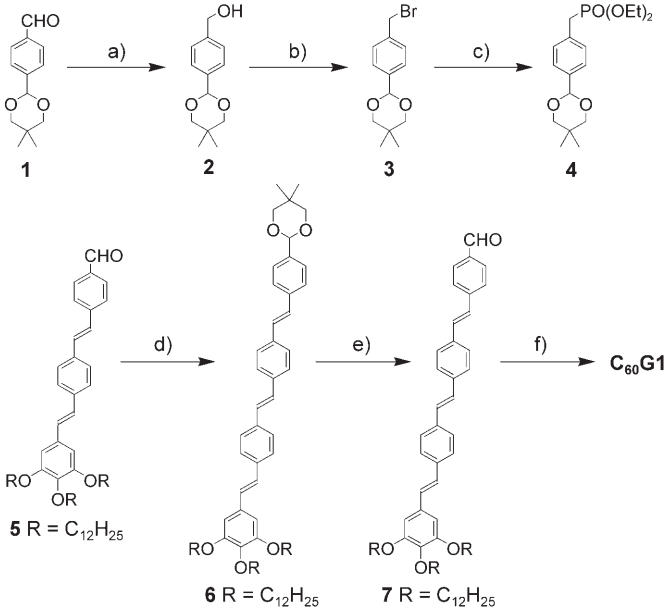

Scheme 1. Preparation of C_{60}**G1**. Reagents and conditions: a) $LiAlH_4$, THF, 0°C (90%); b) PPh_3, CBr_4, THF, room temperature (84%); c) $P(OEt)_3$, 150°C (85%); d) **4**, *t*BuOK, THF, 0°C→RT (88%); e) CF_3CO_2H, CH_2Cl_2, H_2O, room temperature (96%); f) C_{60}, *N*-methylglycine, toluene, Δ (46%).

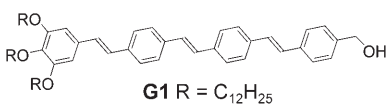

The preparation of bis-phosphonate **13**, the key building block for the preparation of the OPV-terminated phenylenevinylene dendritic wedges, is shown in Scheme 2. 3,5-Dibromobenzaldehyde (**8**) was prepared from 1,3,5-tribromobenzene according to the literature.[25] Reaction of **8** with 2,2-dimethyl-1,3-propanediol in refluxing benzene in the presence of a catalytic amount of *p*-toluenesulfonic acid (*p*-TsOH) afforded **9** in 97% yield. Treatment of **9** with an excess of *t*BuLi in THF followed by quenching with *N*,*N*-dimethylformamide (DMF) and subsequent reduction of the resulting dialdehyde **10** with diisobutylaluminium hydride (DIBAL-H) gave diol **11** in 56% overall yield. Bromination with CBr_4/PPh_3 followed by treatment of the resulting bisbromide **12** with $P(OEt)_3$ under Arbuzov conditions yielded **13** in 66% overall yield.

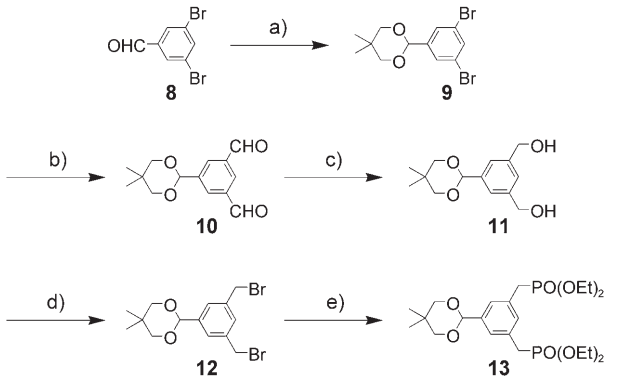

Scheme 2. Preparation of **13**. Reagents and conditions: a) 2,2-dimethyl-1,3-propanediol, C_6H_6, *p*-TsOH cat., Δ, Dean–Stark trap (97%); b) *t*BuLi (4 equiv), THF, −78→0°C, then DMF, −78→0°C, then aq. HCl (2M) (58%); c) diisobutylaluminum hydride (DIBAL-H), CH_2Cl_2, 0°C (97%); d) PPh_3, CBr_4, THF, room temperature (75%); e) $P(OEt)_3$, 150°C (88%).

Reaction of **13** with aldehyde **5** in the presence of *t*BuOK afforded compound **G2** in 91% yield (Scheme 3). Treatment with CF_3CO_2H in CH_2Cl_2/H_2O and subsequent reaction of the resulting aldehyde **14** with C_{60} in the presence of *N*-methylglycine gave C_{60}**G2**. The next-generation dendron **G3** was obtained in 90% yield by reaction of **13** with **14**

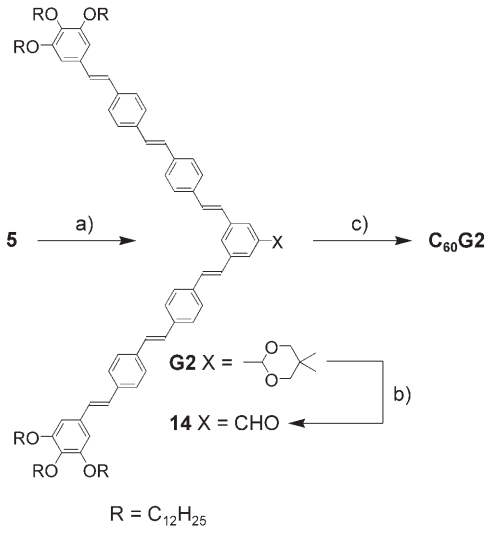

Scheme 3. Preparation of C_{60}**G2**. Reagents and conditions: a) **13**, *t*BuOK, THF, 0°C→RT (91%); b) CF_3CO_2H, CH_2Cl_2, H_2O, room temperature (90%); c) C_{60}, *N*-methylglycine, toluene, Δ (18%).

CHEMISTRY
AN ASIAN JOURNAL

(Scheme 4). Subsequent deprotection with CF_3CO_2H in CH_2Cl_2/H_2O yielded aldehyde **15**, which after reaction with C_{60} and *N*-methylglycine in refluxing toluene gave $\mathbf{C_{60}G3}$ in 25% yield.

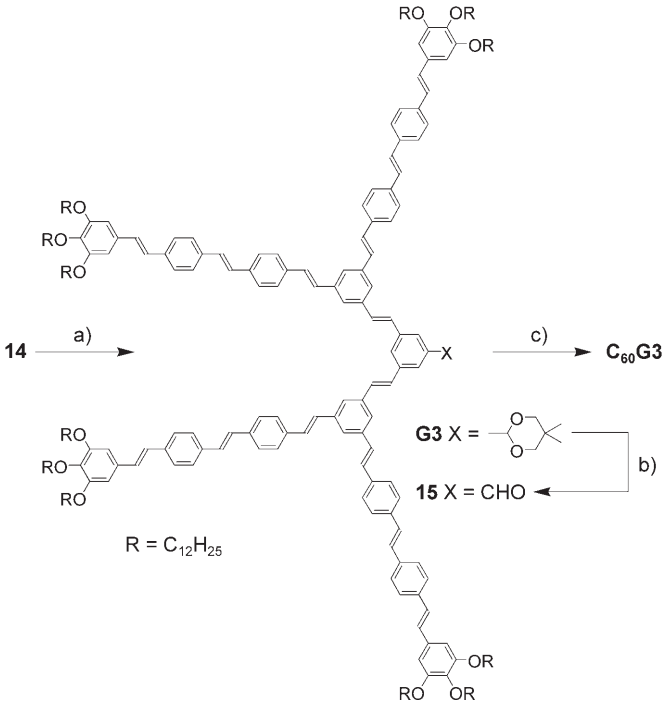

Scheme 4. Preparation of $\mathbf{C_{60}G3}$. Reagents and conditions: a) **13**, *t*BuOK, THF, 0°C→RT (85%); b) CF_3CO_2H, CH_2Cl_2, H_2O, room temperature (90%); c) C_{60}, *N*-methylglycine, toluene, Δ (25%).

The last-generation compound was obtained from **15** by repeating the same synthetic sequence (Scheme 5). Reaction of **13** with **15** and subsequent deprotection with CF_3CO_2H in CH_2Cl_2/H_2O yielded aldehyde **16**. Treatment of **16** with C_{60} and *N*-methylglycine in refluxing toluene finally gave $\mathbf{C_{60}G4}$ in 30% yield.

The structures of fullerodendrimers $\mathbf{C_{60}G1}$–$\mathbf{C_{60}G4}$ were confirmed by analytical and spectroscopic data. The ^{1}H NMR spectra of $\mathbf{C_{60}G1}$ and $\mathbf{C_{60}G2}$ in $CDCl_3$ exhibit the expected features with signals arising from the OPV branches, an AB quartet and a singlet for the pyrrolidine protons, as well as a singlet for the N–CH_3 group. Importantly, the signals corresponding to the protons of the phenyl group directly attached to the pyrrolidine ring are broad at room temperature. As previously described for phenylpyrrolidinofullerene derivatives,[20,26] this indicates restricted rotation of the phenyl substituent on the pyrrolidine ring. This was confirmed by variable-temperature NMR spectroscopic studies, which showed a clear coalescence at about 10°C for the two lower-generation derivatives, and a reversible narrowing was observed in the spectra of $\mathbf{C_{60}G1}$ and $\mathbf{C_{60}G2}$. The ^{1}H NMR spectra of the two highest-generation derivatives $\mathbf{C_{60}G3}$ and $\mathbf{C_{60}G4}$ were more complicated at room temperature. Besides the restricted rotation of the phenyl unit on the pyrrolidine ring, other dynamic effects are also involved. Such behavior has already been reported by Langa et al. for related dendrimers.[20] A variable-temperature study ($CDCl_2CDCl_2$,

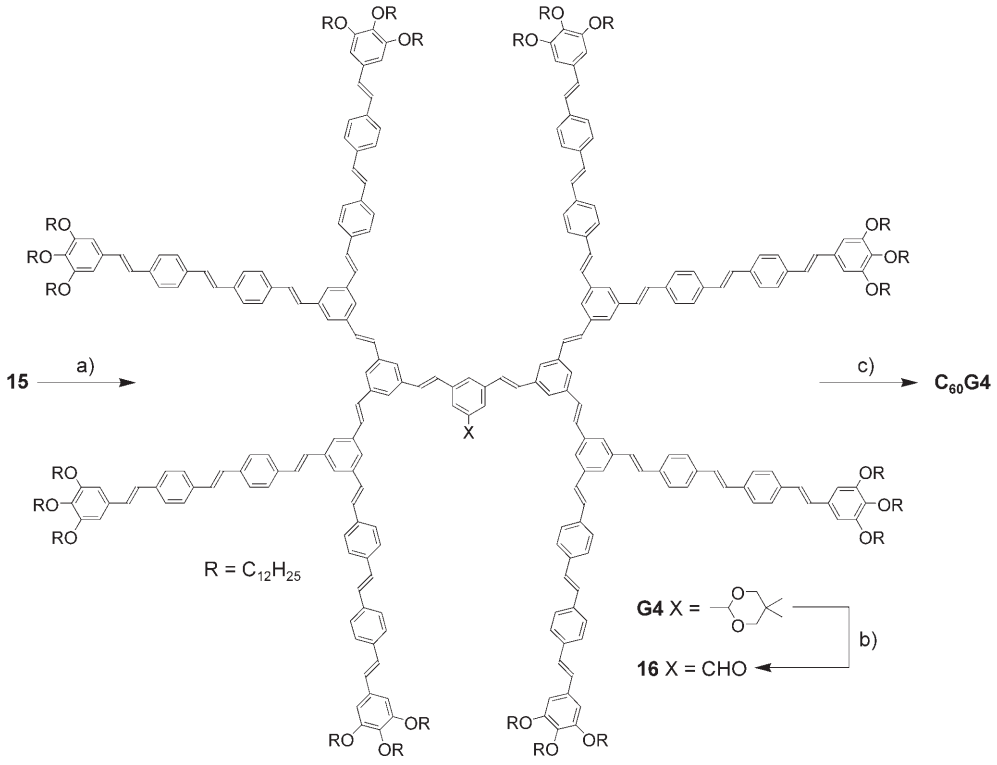

Scheme 5. Preparation of $\mathbf{C_{60}G4}$. Reagents and conditions: a) **13**, *t*BuOK, THF, 0°C→RT (63%); b) CF_3CO_2H, CH_2Cl_2, H_2O, room temperature (95%); c) C_{60}, *N*-methylglycine, toluene, Δ (30%).

400 MHz) showed a perfectly reversible narrowing of all the peaks, and a sharp peak was obtained at 100 °C for both compounds. Finally, the structures of **C_{60}G1**–**C_{60}G4** were confirmed by mass spectrometry. In all cases, the expected molecular-ion peak was clearly observed.

Whereas liquid-crystalline properties have been observed for almost all the dendritic OPV precursors,[27] fullerodendrimers **C_{60}G1**–**C_{60}G4** do not show any mesomorphic behavior. Actually, the π–π interactions among the dendritic wedges capable of stabilizing the mesophases in the unsubstituted precursors are prevented owing to the presence of the bulky fullerene cores in **C_{60}G1**–**C_{60}G4**.

Electronic Absorption Spectra

Reference Compounds

The electronic absorption spectra of the organic conjugated systems **G1**–**G4** in CH_2Cl_2 are shown in Figure 1. The absorption maxima are in the range 390–395 nm and are bathochromically shifted by about 30 nm relative to the shorter analogue with a trimer OPV unit.[28]

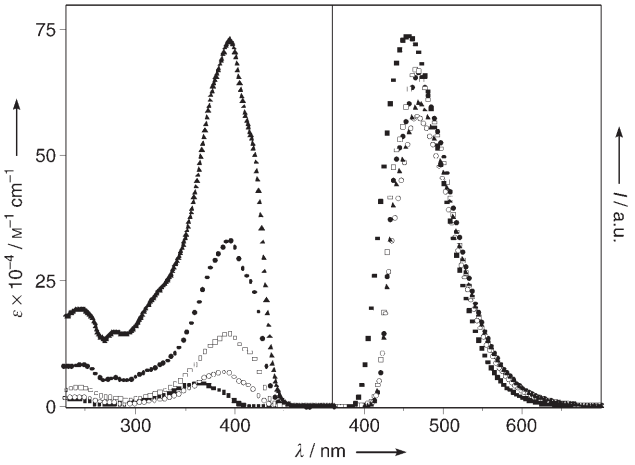

Figure 1. Absorption (left) and fluorescence spectra (right; λ_{ex} = 395 nm, O.D. = 0.2) of **5** (■), **G1** (○), **G2** (□), **G3**, (●), and **G4** (▲). All spectra were recorded at 298 K in CH_2Cl_2.

The trend in the absorption spectra of **G1**–**G4** shows that ramification at the *meta* positions of the phenyl rings does not promote efficient π-electronic conjugation within OPV dendronic subunits, as already observed for oligophenyleneethynylene (OPE) arrays.[29] Practically, **G3**, for example, can be regarded as an assembly of two groups of OPV tetramers sharing a phenyl ring. Similar considerations can be made for the largest molecule **G4**. The absorption spectrum of **C_{60}Ref** shows the well-known features of pyrrolidinofullerenes.[24,28]

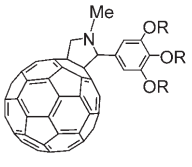

C_{60}Ref R = $C_{12}H_{25}$

Fullerodendrimers

The absorption spectra of the fullerodendrimers **C_{60}G1**–**C_{60}G4** in CH_2Cl_2 are displayed in Figure 2 and clearly show the spectral features of both OPV (UV range) and fulleropyrrolidine (visible window).

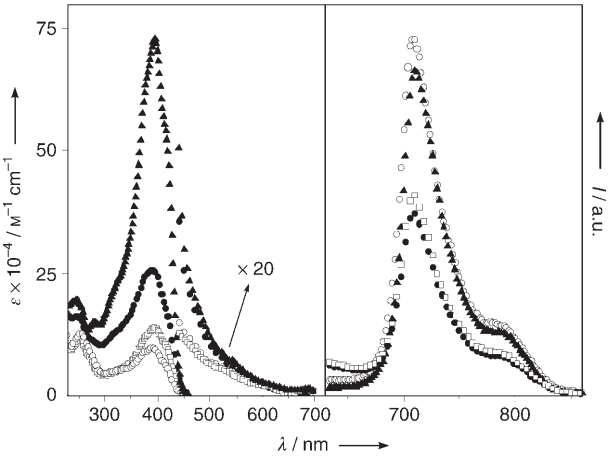

Figure 2. Absorption (left) and fluorescence spectra (right; λ_{ex} = 500 nm, O.D. = 0.2) of **C_{60}G1** (○), **C_{60}G2** (▲), **C_{60}G3**, (●), and **C_{60}G4** (□). All spectra were recorded at 298 K in CH_2Cl_2.

Exact matching with the spectral profiles calculated by summing the absorption spectra of the carbon sphere and the pertinent OPV fragment was not obtained, in line with previous reports.[23] This indicates some degree of intramolecular electronic ground-state interaction between the dendrons and the fullerene core. The difference between calculated and experimental spectra is particularly marked for **C_{60}G3** and **C_{60}G4**, suggesting that electronic interactions are more important when large dendronic networks are present. Molar absorptivities ε ($M^{-1}cm^{-1}$) at the OPV-type band maximum (394 nm) are as follows: 95800 for **C_{60}G1**, 134800 for **C_{60}G2**, 255100 for **C_{60}G3**, and 730400 for **C_{60}G4**. Thus, the relative amount of light captured by the dendronic moiety compared to the fullerene unit ($\varepsilon = 7600\,M^{-1}cm^{-1}$, 394 nm) increases progressively along the series, reaching a ratio of 99:1 for **C_{60}G4**, where incident light is harvested almost exclusively by the OPV-terminated dendrons (antenna effect).

Luminescence Properties and Photoinduced Processes

Reference Compounds

G1–**G4** exhibit intense fluorescence bands in CH_2Cl_2 with λ_{max} in the range of 465–470 nm (Figure 1, Table 1). Strong fluorescence is maintained at 77 K,[30] at which structured spectral profiles were recorded (not shown).

The high fluorescence quantum yields and short singlet excited-state lifetimes at room temperature[23,28] are similar along the series (Table 1). Fulleropyrrolidine **C_{60}Ref** exhibits

Table 1. Luminescence properties of dendrimers in CH_2Cl_2 at 298 K.

	OPV moiety				Fullerene moiety			
	λ_{max} [nm][a]	Φ_{fl} [a]	k_{EnT} [s^{-1}][b]	τ [ns][c]	λ_{max} [nm][d]	Φ_{em} [$\times10^4$][d]	k_{EIT} [s^{-1}][b]	τ [ns][e]
C_{60}Ref	–	–	–	–	710	5.5	–	1.3
G1	464	0.66	–	1.1	–	–	–	–
C_{60}G1	506[f]	0.002	3.0×10^{11}	–[g]	710	5.0	7.7×10^{7}	1.3[h]
G2	464	0.70	–	1.3	–	–	–	–
C_{60}G2	500[f]	0.003	1.8×10^{11}	–[g]	708	4.5	1.7×10^{8}	1.3[h]
G3	468	0.70	–	1.3	–	–	–	–
C_{60}G3	490[f]	0.003	1.8×10^{11}	–[g]	716	2.6	8.6×10^{8}	0.7; 1.8[i]
G4	468	0.67	–	1.4	–	–	–	–
C_{60}G4	468	0.015[j]	3.1×10^{10}[j]	–[g]	716	2.8	7.4×10^{8}	0.7; 1.8[i]

[a] $\lambda_{ex}=390$ nm. [b] Estimated from [Eq. (1)]. [c] $\lambda_{ex}=407$. [d] $\lambda_{ex}=500$ nm. [e] $\lambda_{ex}=637$ nm. [f] Red-shifted due to very low intensity that was strongly affected by instrument noise. [g] Below the temporal resolution of our instrument. [h] The small quenching could not be detected with the time-resolved method. [i] Double exponential decay; the shorter component is attributed to the quenched fullerene unit, the longer is likely to be experimental noise related to the very weak signal and the long accumulation time; a comparable trend has been found for similar measurements in fullerene dyads.[60] [j] Possibly affected by some residual **G4** impurity.

singlet excited-state parameters (Table 1) identical to those of very similar systems reported previously.[23,28]

Fullerodendrimers: OPV Quenching by Energy Transfer

Upon excitation at the OPV band maximum, dramatic quenching of OPV fluorescence was observed for all fullerodendrimers in CH_2Cl_2 (Table 1). The residual fluorescence band in the OPV region was so faint that it was affected by instrument noise and turned out to be artificially red-shifted for **C_{60}G1**–**C_{60}G3** (see Supporting Information). This effect was not observed for **C_{60}G4**, for which the residual luminescence signal was more intense. Excitation spectra taken in the range 300–450 nm at $\lambda_{em}=730$ nm (fullerene fluorescence) show that sensitization of the C_{60} moiety occurred for **C_{60}G1** and **C_{60}G2**, pointing to an OPV→C_{60} singlet–singlet energy-transfer process.[28,31,32] Unfortunately, for the two largest arrays, the OPV residual emission tail covered the weak C_{60} fluorescence and prevented clean excitation spectroscopy. The extent of fullerene fluorescence was reduced by increasing the solvent polarity, owing to competing electron-transfer quenching of the fullerene singlet level,[28,32] as discussed later on. By means of [Eq. (1)],[28,32] it is possible to estimate the rates of the OPV→C_{60} singlet energy-transfer process, which are presented in Table 1. In [Eq. (1)], Φ and Φ_{ref} are the OPV fluorescence quantum yields of the multicomponent arrays and the reference compounds, respectively, and τ_{ref} is the OPV singlet lifetime of the latter.

$$k_{EnT}=\frac{\left(\frac{\Phi_{ref}}{\Phi}-1\right)}{\tau_{ref}} \qquad (1)$$

Fullerodendrimers: Size Dependence of C_{60} Fluorescence Spectra

Direct excitation of the C_{60} moiety of **C_{60}G1**–**C_{60}G4** in CH_2Cl_2 at $\lambda\geq430$ nm produced the fluorescence spectra in Figure 2. Relative to the pyrrolidinofullerene reference molecule, a progressive decrease in fluorescence quantum yield was found, and the quenching rates are as follows: 10% (**C_{60}G1**), 25% (**C_{60}G2**), and 55% (**C_{60}G3**, **C_{60}G4**). For the three largest dendrimers, the observed quenching was substantial and well within the experimental uncertainty; for **C_{60}G3** and **C_{60}G4**, shorter singlet lifetimes were measured accordingly (Table 1). Due to energetic reasons (see below), the only possible quenching mechanism for the C_{60} singlet level is **G*n***→C_{60} electron transfer, in line with the behavior of several other C_{60}–OPV arrays investigated by us and others.[28,31,32] By means of [Eq. (1)], the rate of electron transfer can be estimated from fluorescence data (Table 1).

The fact that the electron-transfer rate is dependent on the OPV size is somewhat surprising if one considers that the oxidation potential of the OPV unit is not expected to change substantially along the series because the oxidation process is centered at the terminal methoxybenzene unit,[33] which is identical for the whole family investigated here. On the other hand, the fullerene reduction behavior is also not expected to change appreciably by linking OPV units to pyrrolidinofullerenes.[28] From the first reduction and oxidation potential of **C_{60}G1**–**C_{60}G4**,[34] the free energy of the charge-separated state C_{60}^{-}–**G*n*$^{+}$** is estimated to be 1.65 ± 0.02 eV in CH_2Cl_2.[35] The relative position of this level with respect to the localized lowest singlet and triplet states of the OPV and C_{60} moieties can be seen in the energy level diagram shown in Figure 3.

It is clear from Figure 3 that, for **C_{60}G1**–**C_{60}G4** in CH_2Cl_2, **G*n***→C_{60} electron transfer from the fullerene singlet is slightly exergonic ($\Delta G_{CS}\approx0.07$ eV) in all cases. Such a small change in free energy is critical, if related to the activation barrier for electron transfer, $\Delta G_{CS}^{\#}$, which, according to the classical Marcus approach,[36] depends on the reaction thermodynamics and reorganization energy λ [Eq. (2)]:

$$\Delta G_{CS}^{\#}=\frac{(\Delta G_{CS}+\lambda)^2}{4\lambda} \qquad (2)$$

We have shown previously that, for a system structurally similar to **C_{60}G1** and characterized by a shorter donor moiety (OPV trimer), the activation barrier for electron transfer in CH_2Cl_2 is relatively high ($\Delta G^{\#}=0.22$ eV) and able to prevent a slightly exergonic ($\Delta G_{CS}\approx0.03$ eV) electron transfer.[28] A very similar activation barrier is present here for **C_{60}G1**, in which minor (if any) fullerene fluorescence quenching is detected. By contrast, **C_{60}G2**, **C_{60}G3**, and **C_{60}G4** undergo electron transfer in CH_2Cl_2 (Figure 2, Table 1), and this points to lower $\Delta G^{\#}$ values, which implies,

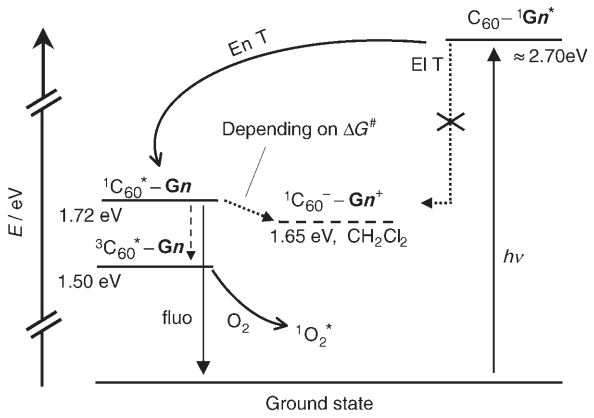

Figure 3. Energy diagram showing the energy levels of the lowest excited states of **C_{60}G1**–**C_{60}G4** and the light-induced intercomponent processes following light excitation of the OPV subunit. The energy of the charge-separated state is determined with the redox potentials and is the same along the fullerodendrimer series. Pyrrolidinofullerene energy levels are known,[28] whereas the OPV singlet-state position was evaluated from the highest-energy feature of the fluorescence spectra at 77 K. For more details, see text. En T = energy transfer, El T = electron transfer.

given the virtually identical ΔG_{CS} values, a lower reorganization energy λ. This parameter is the result of two contributions [Eq. (3)]:[36]

$$\lambda = \lambda_i + \lambda_e \quad (3)$$

where λ_i and λ_e are the internal (nuclear rearrangement) and external (solvent factor) reorganization energies. For C_{60} dyads, λ_i is in the range 0.2–0.3 eV,[32,37,38] whereas λ_e can be estimated from the following equation, assuming a spherical shape of the donor and acceptor partner [Eq. (4)]:[39,40]

$$\lambda_e = \frac{q^2}{4\pi\varepsilon_0}\left(\frac{1}{2r^+}+\frac{1}{2r^-}-\frac{1}{R_{DA}}\right)\left(\frac{1}{n^2}-\frac{1}{\varepsilon_s}\right) \quad (4)$$

where q is the electron charge, ε_0 is the vacuum permittivity, R_{DA} is the center-to-center distance of the positive and negative charges in the charge-separated state, r^+ and r^- are the radii of the oxidized and reduced species, respectively, and n and ε_s are the refractive index and dielectric constant of the solvent, respectively.

Given the increasing complexity of large dendritic structures, it is not straightforward to quantitatively relate the observed electron transfer with the above equations, also because the donor moieties in **C_{60}G1**–**C_{60}G4** are not spherical and are structurally different from one another. For instance, the r^+ value can hardly be estimated, and perhaps even compared, among the various dyads, owing to the increasing ramification of the donor moiety. However, on a qualitative basis, the following considerations can be made: 1) The donor–acceptor (DA) distance between the C_{60} core and the closest trimethoxybenzene OPV terminal unit decreases progressively with dendrimer size; molecular-modeling calculations give the shortest DA distances as 23.5, 18.2, 15.9, and 14.5 Å from **C_{60}G1** to **C_{60}G4**.[41] 2) Partial delocalization of the positive charge among the acceptor trimethoxybenzene OPV terminal could occur from **C_{60}G2** onwards, leading to a bigger r^+ value. Both factors concur to promote a decrease in external reorganization energy when the fullerodendrimer structure grows, according to [Eq. (4)]. This prompts a decrease in the activation energy and favors electron transfer in larger structures, as observed experimentally. The closest distance among electron donor/acceptor couples and the more-compact structure in larger dendrimers is also in line with the differences in ground-state absorption spectra, which do not match the sum of the spectra of the component units (see above).

Fullerodendrimers: Solvent Dependence of C_{60} Fluorescence Spectra

As discussed above, the charge-separated state and the lowest fullerene singlet level are almost isoenergetic for all fullerodendrimers in CH_2Cl_2 (Figure 3). Thus, it is reasonable to expect that a slight tuning of the solvent polarity can substantially affect the extent of electron transfer.[28] To test this hypothesis, we also investigated the whole series of dyads in toluene (TOL) and benzonitrile (BN), which are less and more polar than CH_2Cl_2 (DCM), respectively. As an example of the observed trend, the C_{60} fluorescence spectra of **C_{60}G2** recorded in the three solvents are displayed in Figure 4 (top). The results of the whole fullerodendrimer series in terms of relative fluorescence intensity versus solvent polarity are gathered in Figure 5 (top).

A clear trend showing an enhanced fullerene singlet quenching, that is, an enhanced **Gn**→C_{60} electron transfer, was found for all compounds. In BN (most polar), the three largest dendrimers exhibited extensive electron transfer (>50%), whereas the efficiency in **C_{60}G1** is lower (≈30%). A rather interesting and unexpected result is that the largest systems **C_{60}G3** and **C_{60}G4** undergo electron transfer with about 40% efficiency also in nonpolar TOL. This is, to the best of our knowledge, unprecedented in dyads made of C_{60} and organic conjugated moieties[16] and highlights once again the importance of structural factors in addressing light-induced processes in complex arrays.[15,31] Practically, what is thermodynamically forbidden in simple systems may become allowed in complex architectures in which the same donor–acceptor partners can assume different relative positions and distances or experience modified local polarities.[31,42] In Figure 5 (bottom), the trend in solvent polarity is described as a function of dendrimer ramification, showing that the largest differences are found up to the third-generation dendrimer **C_{60}G3**, after which a plateau is reached. Importantly, the trends in C_{60} fluorescence intensity are the same, within a 10% experimental uncertainty, both by exciting the C_{60} moiety (λ_{exc} > 450 nm) and the OPV unit (395 nm). This unambiguously confirms that the singlet excited state of the OPV unit does not trigger electron transfer, but simply sensitizes the C_{60} singlet level by energy transfer,[28] as discussed above.

CHEMISTRY
AN ASIAN JOURNAL

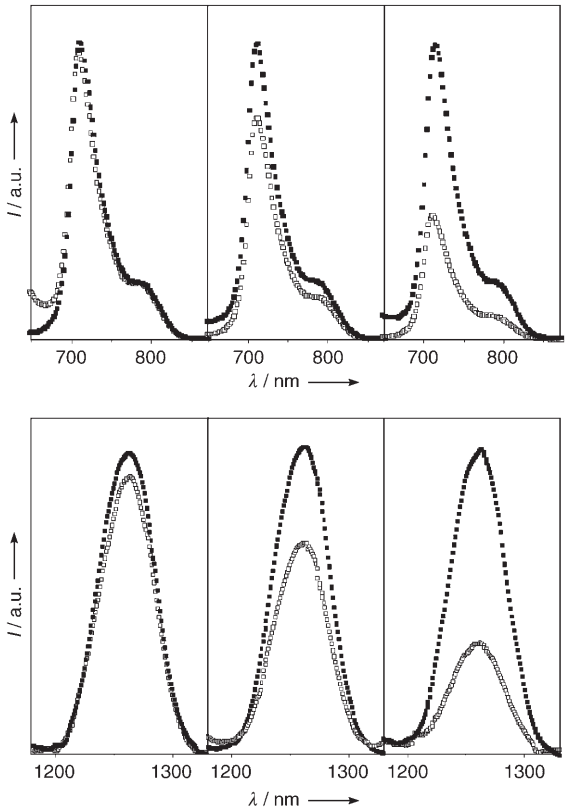

Figure 4. Top: C_{60} fluorescence spectra of **C_{60}G2** (□) in TOL (left), DCM (middle), and BN (right) at 298 K relative to that of **C_{60}Ref** (■) (λ_{ex} = 500 nm, O.D. = 0.3). Bottom: Sensitized singlet oxygen luminescence spectra of **C_{60}G2** (□) in TOL (left), DCM (middle), and BN (right) at 298 K relative to that of **C_{60}Ref** (■) (λ_{ex} = 390 nm, O.D. = 0.5).

Triplet Behavior

To gain further insight into the photophysical processes following light excitation of **C_{60}G1**–**C_{60}G4**, the yield of formation of the lowest fullerene triplet excited state in the three solvents was measured. To this end we took advantage of the singlet oxygen sensitization process brought about by the lowest triplet state of fullerenes according to [Eq. (5)]:[16,43,44]

$$C_{60} \xrightarrow{h\nu} {}^1C_{60}^* \xrightarrow{ISC} {}^3C_{60}^* \xrightarrow{O_2} C_{60} + {}^1O_2^* \qquad (5)$$

where ISC denotes intersystem crossing and $^1O_2$* stands for $O_2(^1\Delta_g)$, commonly termed "singlet oxygen". The excited $^1O_2$* state deactivates to the ground state, giving rise to a characteristic IR emission band centered at λ = 1268 nm.[45] The quantum yield of singlet oxygen sensitization (Φ_Δ) and of fullerene triplet formation (Φ_T) are found to be identical for C_{60}, for its closed-cage[46] and open-cage[47] derivatives, as well as for higher fullerenes like C_{70}[48] and C_{76}.[49] Therefore, the value of Φ_Δ, which is proportional to the intensity of the sensitized IR emission of $^1O_2$*,[42,50] can be used as an indirect measurement of Φ_T for all fullerenes.[28,51] The sensitized singlet oxygen luminescence bands of **C_{60}G2** in TOL, DCM, and BN, with **C_{60}Ref** as internal reference in all cases, is shown in Figure 4 (bottom). The relative $^1O_2$* luminescence intensity ratios (**C_{60}Ref**/**C_{60}G2**) obtained by exciting both compounds at 395 nm (OPV moiety) and above 450 nm (C_{60} subunit) were identical.

Importantly, the spectra of Figure 4 show that the relative amount of fullerene singlet formed (monitored by C_{60} fluorescence) is identical to that of triplet (monitored by sensitized $^1O_2$ luminescence) in any solvent.[28] Triplet lifetimes of **C_{60}Ref** and **C_{60}G2** were identical in air-equilibrated and air-free solution (698 ns and 22 μs, respectively).[52] This shows that no fullerene triplet quenching occurs in the fullerodendrimers and the lower yield of triplet formation is simply due to singlet depletion by electron transfer (see above); triplet excited-state dyad molecules undergo regular deactivation. The parallel trend in fluorescence and singlet oxygen sensitization spectra is found also for the other fullerodendrimers in all the solvents investigated, and the above rationale is extended to the whole family **C_{60}G1**–**C_{60}G4**. As an example, the emission spectra of **C_{60}G4**, recorded with a near-IR (NIR)-sensitive detector that is able to record both the fullerene fluorescence and the singlet oxygen

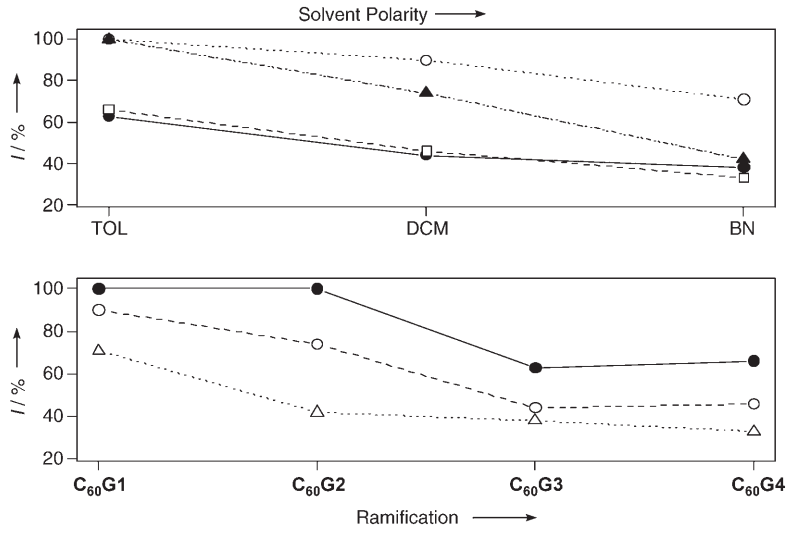

Figure 5. Top: Relative C_{60} fluorescence intensity of **C_{60}G1** (○), **C_{60}G2** (▲), **C_{60}G3**, (●), and **C_{60}G4** (□) as a function of solvent polarity. Bottom: Relative C_{60} fluorescence intensity as a function of dendrimer ramification/size for dendrimers in TOL (●), DCM (○), and BN (△). The reference value 100, recorded for each experiment, corresponds to the fluorescence intensity of the pyrrolidinofullerene **C_{60}Ref** under the same experimental conditions (see top panel of Figure 4 as an example).

luminescence, are shown in Figure 6. One can see the decrease in intensity with solvent polarity, as well as the unexpected luminescence quenching of the largest fullerodendrimer **C_{60}G4** in low-polarity toluene as described above.

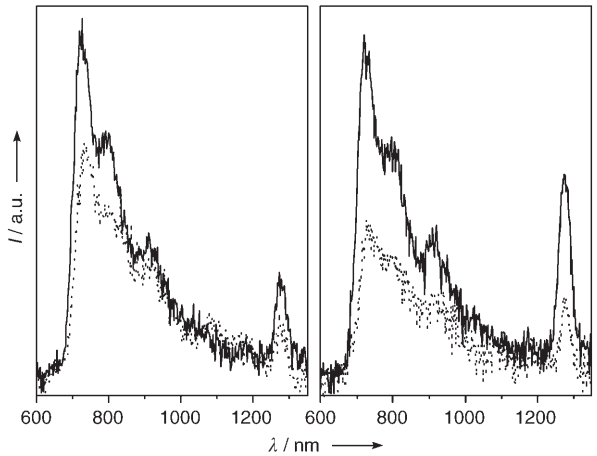

Figure 6. Luminescence spectra ($\lambda_{ex}=500$ nm, O.D.$=0.3$) of **C_{60}G4** (full line) and **C_{60}Ref** (dotted line) in TOL (left) and DCM (right) recorded with a NIR-sensitive photomultiplier detector, showing the parallel decrease of C_{60} fluorescence and sensitized singlet oxygen luminescence; the same trend is observed for all compounds in all solvents. The highest relative intensity of $^1O_2$* emission in DCM compared to TOL reflects the intrinsic higher yield of the radiative process in the former solvent. By contrast, there is virtually no difference in C_{60} fluorescence yield between the two solvents.

Finally, in an attempt to detect the charge-separated state C_{60}^{-}–**G*n*$^{+}$**, we recorded transient absorption spectra in the visible/NIR region up to 1200 nm. Figure 7 shows the spectra of **C_{60}G1** in TOL and **C_{60}G3** in BN. No trace of fulleropyrrolidine anion around 1000 nm[32,53] or OPV cation in the visible/NIR region[32,54] was found down to a temporal window of 10 ns because the charge-separated state is much more short-lived, as found for other C_{60}–OPV dyad systems.[55] However, the high intensity of the spectrum of **C_{60}G3** relative to **C_{60}G1** is pretty much in line with that of the singlet oxygen spectra, thus confirming the above illustrated rationalization of light-induced processes.

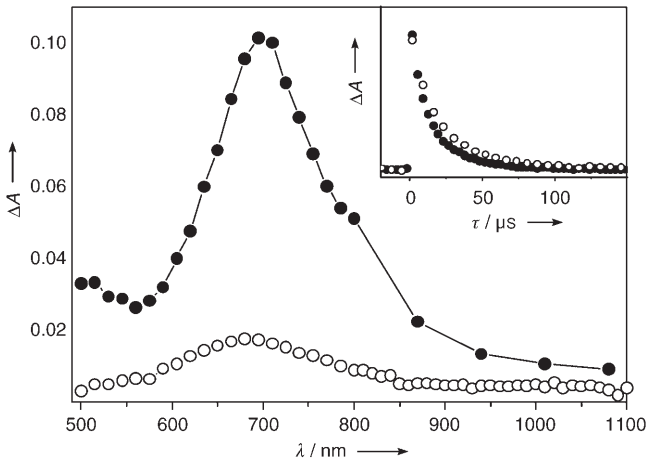

Figure 7. Transient absorption spectra of **C_{60}G1** in degassed TOL (○) and **C_{60}G3** in degassed BN (●) at 298 K upon laser excitation at 532 nm ($E\approx5$ mJ per pulse). The spectra were recorded at a delay of 0.25 μs following excitation. The inset shows the time profile of ΔA (700 nm) from which the spectral kinetic data were obtained; the fitting is monoexponential and gives a lifetime of 14.1 and 20.2 μs for **C_{60}G1** and **C_{60}G3**, respectively. Such triplet lifetime values do not change when the decay is examined at 1000 nm.

Conclusions

A series of dyads with an increasingly large dendritic OPV moieties and an identical pyrrolidinofullerene core has been prepared. The molecular design of these architectures prompts a unique ensemble of electronic and spectroscopic properties. **C_{60}G1**–**C_{60}G4** are characterized by an increasingly efficient light-harvesting moiety (OPV), which quantitatively conveys the excitation energy to the carbon sphere. Eventually, this process results in an ultrafast OPV→C_{60} charge separation and recombination. Branching of the OPV dendritic subunits at the *meta* position of the phenylene rings does not promote effective π delocalization within the electron-donor OPV moiety; its oxidation potential is unchanged with molecular size. Consequently, owing to the invariance of the acceptor carbon sphere, the energy of the charge-separated state is virtually the same along the series, and the differences in the extent of electron transfer as a function of OPV ramification or solvent polarity are attributed to structural factors only. The observed regular trends are related to electron-transfer theory, albeit only on a qualitative basis, owing to the high complexity of fullerodendrimer structures. The most relevant results are found for the largest dendrimers **C_{60}G3** and **C_{60}G4**, which exhibit, in a given solvent, the largest electron-transfer efficiency and, quite unexpectedly, show evidence of charge separation even in nonpolar toluene. These results demonstrate once again the crucial role played by structural factors in fostering charge separation within complex fullerene architectures.[31] Notably, this is somehow reminiscent of the concept that local nanomorphology is a key factor for successful exciton dissociation and efficient conversion of light energy in plastic photovoltaic devices made with fullerene materials.[56]

Experimental Section

General Methods

Reagents and solvents were purchased at reagent grade and used without further purification. Compounds **1**,[23] **5**,[33] and **8**[25] were prepared as previously reported. The experimental details for the preparation of all the compounds are reported in the Supporting Information. NMR spectra were recorded on a Bruker AC 200 (200 MHz) or a Bruker AM 400 (400 MHz) spectrometer with solvent peaks as reference. FAB MS was performed on a ZA HF instrument with 4-nitrobenzyl alcohol as matrix. MALDI-TOF MS was performed on a Brucker BIFLEX™ mass spec-

trometer under previously reported conditions.[42] Elemental analyses were performed by the analytical service at the Institut Charles Sadron, Strasbourg.

Synthesis

C_{60}G3: A mixture of **15** (520 mg, 0.13 mmol), C_{60} (110 mg, 0.15 mmol), and sarcosine (100 mg, 1.10 mmol) in toluene (120 mL) was heated under reflux and Ar for 24 h. After cooling, the resulting solution was evaporated to dryness. Column chromatography (SiO_2, hexane/toluene = 1:1) followed by gel permeation chromatography (Biorads, biobeads SX-1, CH_2Cl_2) gave **C_{60}G3** (125 mg, 25%) as a dark-brown glassy product. ^{1}H NMR (400 MHz, 100 °C, $C_2D_2Cl_4$): δ = 8.02 (s, 2H), 7.77 (s, 1H), 7.50 (m, 38H), 7.34 (AB, J = 17 Hz, 4H), 7.24 (AB, J = 17 Hz, 8H), 7.18 (s, 8H), 7.03 (AB, J = 17 Hz, 8H), 6.78 (s, 8H), 5.14 (d, J = 10 Hz, 1H), 5.12 (s, 1H), 4.42 (d, J = 10 Hz, 1H), 4.09 (t, J = 6 Hz, 16H), 4.06 (t, J = 6 Hz, 8H), 2.83 (s, 3H), 1.83 (m, 24H), 1.50–1.20 (m, 216H), 0.89 ppm (t, J = 6 Hz, 36H); ^{13}C NMR (100 MHz, $C_2D_2Cl_4$): δ = 153.3, 147–140 (br), 138.0, 136.6, 136.2, 132.1, 128.8, 128.1, 127.8, 126.8, 126.7, 104.7. 68.8, 31.8, 30.2, 29.9, 29.65, 29.6, 29.5, 29.3, 29.25, 26.0, 22.6, 14.1 ppm; MS (MALDI-TOF): calcd for $C_{325}H_{384}NO_{12}$: 4496.6 $[M+H]^+$; found: 4498; elemental analysis: calcd (%) for $C_{325}H_{383}NO_{12}CHCl_3$: C 84.84, H 8.39, N 0.30; found: C 85.09, H 8.53, N 0.29.

C_{60}G4: A mixture of **16** (600 mg, 0.079 mmol), C_{60} (114 mg, 0.15 mmol), and sarcosine (70 mg, 0.79 mmol) in toluene (120 mL) was heated under reflux and Ar for 24 h. After cooling, the resulting solution was evaporated to dryness. Column chromatography (SiO_2, hexane/toluene = 1:1) followed by gel permeation chromatography (Biorads, biobeads SX-1, CH_2Cl_2) gave **C_{60}G4** (198 mg, 30%) as a dark-brown glassy product. ^{1}H NMR (400 MHz, 100 °C, $C_2D_2Cl_4$): δ = 7.70–6.90 (m, 70H), 6.73 (m, 8H), 4.04 (m, 24H), 3.03 (s, 3H), 1.83 (m, 24H), 1.28 (m, 216H), 0.89 ppm (t, J = 6 Hz, 36H); MS (MALDI-TOF): calcd for $C_{597}H_{767}N_1O_{24}K$: 8380.7 $[M+K]^+$; found: 8380; calcd for $C_{537}H_{767}NO_{24}$: 7620.9 $[M-C_{60}]^+$; found: 7620; elemental analysis: calcd (%) for $C_{597}H_{767}N_1O_{24}$: C 85.96, H 9.27, N 0.17; found: C 85.57, H 9.12, N 0.16.

Photophysical Measurements

Absorption spectra were recorded with a Perkin–Elmer λ40 spectrophotometer. Emission spectra were obtained with an Edinburgh FLS920 spectrometer (continuous 450-W Xe lamp) equipped with a Peltier-cooled Hamamatsu R928 photomultiplier tube (PMT; 185–850 nm) or a Hamamatsu R5509-72 supercooled PMT (193 K, 400–1700 nm). Corrected spectra were obtained by a calibration curve supplied by the instrument manufacturer. Emission quantum yields were determined according to the approach described by Demas and Crosby[57] by using air-equilibrated [Ru(bipyridine)$_3$Cl$_2$] (Φ_{em} = 0.028 in air-equilibrated water)[58] or quinine sulfate (Φ_{em} = 0.546 in 1 N H_2SO_4)[59] as standards. Emission lifetimes were determined with the time-correlated single photon counting technique by using an Edinburgh FLS920 spectrometer equipped with a laser diode head as excitation source (1 MHz repetition rate, λ_{ex} = 407 or 637 nm, time resolution upon deconvolution = 200 ps) and a Hamamatsu R928 PMT as detector. Transient absorption spectra in the nanosecond–microsecond time domain were obtained by using the nanosecond flash photolysis apparatus Proteus by Ultrafast Systems LLC. The excitation source was the second harmonic (532 nm) of a Continuum Surelite II Nd:YAG laser with 5-ns pulse duration at 5 mJ per pulse. Light signals were passed through a Chromex/Bruker 250IS monochromator (equipped with two gratings blazed at 500 or 1000 nm) and collected on a high-speed Silicon (DET210) or InGaAs (DET410) Thorlabs detector in the visible (400–800 nm) or NIR (400–1700 nm) region, respectively. The signal was then amplified by means of a variable-gain wideband voltage amplifier (Femto DHPVA-200) interfaced with a Tektronix TDS 3032B digital oscilloscope connected to a PC with the acquisition software Proteus. The probe light source was a 150-W continuous wave Xe arc lamp (Spectra Physics 69907). Triplet lifetimes were obtained by averaging 264 different decays recorded around the maximum of the absorption peak (680–720 nm). The samples were placed in fluorimetric 1-cm path cuvettes and, when necessary, purged from oxygen by at least four freeze–thaw–pump cycles.

All measurements were carried out in spectroscopy-grade solvents used without further purification. Experimental uncertainties are estimated to be 8% for lifetime determinations, 20% for emission quantum yields, 5% for relative emission intensities in the NIR, and 1 nm and 5 nm for absorption and emission peaks, respectively.

Acknowledgements

This work was supported by the CNR (commessa PM-P04-ISTM-C1-ISOF-M5, Componenti Molecolari e Supramolecolari o Macromolecolari con Proprietà Fotoniche ed Optoelettroniche), the CNRS, the French Ministry of Research (ACI Jeunes Chercheurs), and the EU through the RTN contract "FAMOUS" No. HPRN-CT-2002–00171. J.-F.E. thanks DGA for his research fellowships. We further thank L. Oswald for technical help, Dr. B. Heinrich for his help for the characterization of the liquid-crystalline derivatives, M. Schmitt for high-field NMR measurements, and Prof. J.-P. Gisselbrecht for electrochemical measurements.

[1] V. Balzani, S. Campagna, G. Denti, A. Juris, S. Serroni, M. Venturi, *Acc. Chem. Res.* **1998**, *31*, 26–34.
[2] V. Balzani, P. Ceroni, A. Juris, M. Venturi, S. Campagna, F. Puntoriero, S. Serroni, *Coord. Chem. Rev.* **2001**, *219*, 545–572.
[3] A. Adronov, J. M. J. Frechet, *Chem. Commun.* **2000**, 1701–1710.
[4] M. Fischer, F. Vögtle, *Angew. Chem.* **1999**, *111*, 934–955; Angew. Chem. Int. Ed. **1999**, 38, 884–905.
[5] G. Bergamini, P. Ceroni, M. Maestri, V. Balzani, S. K. Lee, F. Vögtle, *Photochem. Photobiol. Sci.* **2004**, *3*, 898–905.
[6] G. Bergamini, C. Saudan, P. Ceroni, M. Maestri, V. Balzani, M. Gorka, S. K. Lee, J. van Heyst, F. Vogtle, *J. Am. Chem. Soc.* **2004**, *126*, 16466–16471.
[7] A. D′Aleo, R. M. Williams, F. Osswald, P. Edamana, U. Hahn, J. van Heyst, F. D. Tichelaar, F. Vogtle, L. De Cola, *Adv. Funct. Mater.* **2004**, *14*, 1167–1177.
[8] J. P. Cross, M. Lauz, P. D. Badger, S. Petoud, *J. Am. Chem. Soc.* **2004**, *126*, 16278–16279.
[9] T. Hasobe, P. V. Kamat, M. A. Absalom, Y. Kashiwagi, J. Sly, M. J. Crossley, K. Hosomizu, H. Imahori, S. Fukuzumi, *J. Phys. Chem. B* **2004**, *108*, 12865–12872.
[10] D. Gust, T. A. Moore, A. L. Moore, *Acc. Chem. Res.* **2001**, *34*, 40–48.
[11] L. C. Sun, L. Hammarström, B. Åkermark, S. Styring, *Chem. Soc. Rev.* **2001**, *30*, 36–49.
[12] J. Baffreau, L. Perrin, S. Leroy-Lhez, P. Hudhomme, *Tetrahedron Lett.* **2005**, *46*, 4599–4603.
[13] R. Gomez, J. L. Segura, N. Martin, *Org. Lett.* **2005**, *7*, 717–720.
[14] A. J. Berresheim, M. Muller, K. Mullen, *Chem. Rev.* **1999**, *99*, 1747–1785.
[15] J.-F. Nierengarten, N. Armaroli, G. Accorsi, Y. Rio, J.-F. Eckert, *Chem. Eur. J.* **2003**, *9*, 36–41.
[16] N. Armaroli in *Fullerenes: From Synthesis to Optoelectronic Properties* (Eds.: D. M. Guldi, N. Martin), Kluwer Academic Publishers, Dordrecht, **2002**, pp. 137–162.
[17] G. Accorsi, N. Armaroli, J.-F. Eckert, J.-F. Nierengarten, *Tetrahedron Lett.* **2002**, *43*, 65–68.
[18] J. L. Segura, R. Gomez, N. Martin, C. P. Luo, A. Swartz, D. M. Guldi, *Chem. Commun.* **2001**, 707–708.
[19] D. M. Guldi, A. Swartz, C. P. Luo, R. Gomez, J. L. Segura, N. Martin, *J. Am. Chem. Soc.* **2002**, *124*, 10875–10886.
[20] F. Langa, M. J. Gómez-Escalonilla, E. Díez-Barra, J. C. García-Martínez, A. de la Hoz, J. Rodríguez-López, A. González-Cortés, V. López-Arza, *Tetrahedron Lett.* **2001**, *42*, 3435–3438.
[21] A. G. Avent, P. R. Birkett, F. Paolucci, S. Roffia, R. Taylor, N. K. Wachter, *J. Chem. Soc. Perkin Trans. 2* **2000**, 1409–1414.
[22] M. Schwell, N. K. Wachter, J. H. Rice, J. P. Galaup, S. Leach, R. Taylor, R. V. Bensasson, *Chem. Phys. Lett.* **2001**, *339*, 29–35.

[23] J.-F. Eckert, J.-F. Nicoud, J.-F. Nierengarten, S.-G. Liu, L. Echegoyen, F. Barigelletti, N. Armaroli, L. Ouali, V. Krasnikov, G. Hadziioannou, *J. Am. Chem. Soc.* **2000**, *122*, 7467–7479.
[24] M. Prato, M. Maggini, *Acc. Chem. Res.* **1998**, *31*, 519–526.
[25] L. S. Chen, G. J. Chen, C. Tamborski, *J. Organomet. Chem.* **1981**, *215*, 281–291.
[26] P. de la Cruz, A. de la Hoz, L. M. Font, F. Langa, M. C. Pérez-Rodríguez, *Tetrahedron Lett.* **1998**, *39*, 6053–6056.
[27] The liquid-crystalline and thermal properties of **14**, **G3**, **15**, **G4**, and **16** were examined by polarized optical microscopy and differential scanning calorimetry (DSC). In all cases, the optical textures obtained from cooling the samples from the isotropic phase were characteristic of columnar mesophases. The transition temperatures are indicated in the Experimental Section.
[28] N. Armaroli, G. Accorsi, J.-P. Gisselbrecht, M. Gross, V. Krasnikov, D. Tsamouras, G. Hadziioannou, M. J. Gomez-Escalonilla, F. Langa, J.-F. Eckert, J.-F. Nierengarten, *J. Mater. Chem.* **2002**, *12*, 2077–2087.
[29] J.-F. Nierengarten, S. Zhang, A. Gegout, M. Urbani, N. Armaroli, G. Marconi, Y. Rio, *J. Org. Chem.* **2005**, *70*, 7550–7557.
[30] J. S. de Melo, J. Pina, H. D. Burrows, S. Brocke, O. Herzog, E. Thorn-Csanyi, *Chem. Phys. Lett.* **2004**, *388*, 236–241.
[31] M. Gutierrez-Nava, G. Accorsi, P. Masson, N. Armaroli, J.-F. Nierengarten, *Chem. Eur. J.* **2004**, *10*, 5076–5086.
[32] E. Peeters, P. A. van Hal, J. Knol, C. J. Brabec, N. S. Sariciftci, J. C. Hummelen, R. A. J. Janssen, *J. Phys. Chem. B* **2000**, *104*, 10174–10190.
[33] T. Gu, P. Ceroni, G. Marconi, N. Armaroli, J.-F. Nierengarten, *J. Org. Chem.* **2001**, *66*, 6432–6439.
[34] The electrochemical properties of **C_{60}G1**–**C_{60}G4** were investigated by cyclic voltammetry in solutions of CH_2Cl_2 containing Bu_4NPF_6 (0.1 M). For all the compounds, the first reduction centered on the fullerene core was observed at about −1.09 V relative to Fc^+/Fc and the first oxidation centered on the OPV dendritic branch at about +0.55 V relative to Fc^+/Fc.
[35] V. Balzani, F. Scandola, *Supramolecular Photochemistry*, Ellis Horwood, Chichester, **1991**, pp. 44–45.
[36] R. A. Marcus, N. Sutin, *Biochim. Biophys. Acta* **1985**, *811*, 265–322.
[37] R. M. Williams, J. M. Zwier, J. W. Verhoeven, *J. Am. Chem. Soc.* **1995**, *117*, 4093–4099.
[38] M. Holler, F. Cardinali, H. Mamlouk, J.-F. Nierengarten, J.-P. Gisselbrecht, M. Gross, Y. Rio, F. Barigelletti, N. Armaroli, *Tetrahedron* **2006**, *62*, 2060–2073.
[39] R. M. Williams, M. Koeberg, J. M. Lawson, Y. Z. An, Y. Rubin, M. N. Paddon-Row, J. W. Verhoeven, *J. Org. Chem.* **1996**, *61*, 5055–5062.
[40] J. Kroon, J. W. Verhoeven, M. N. Paddon-Row, A. M. Oliver, *Angew. Chem.* **1991**, *103*, 1398–1401; *Angew. Chem. Int. Ed. Engl.* **1991**, *30*, 1358–1361.
[41] Distances measured by MM2-CS, Chem3D Ultra, CambridgeSoft, Cambridge (USA), **2000**.
[42] Y. Rio, G. Accorsi, H. Nierengarten, C. Bourgogne, J.-M. Strub, A. Van Dorsselaer, N. Armaroli, J.-F. Nierengarten, *Tetrahedron* **2003**, *59*, 3833–3844.
[43] R. R. Hung, J. J. Grabowski, *J. Phys. Chem.* **1991**, *95*, 6073–6075.
[44] J. W. Arbogast, A. P. Darmanyan, C. S. Foote, Y. Rubin, F. N. Diederich, M. M. Alvarez, S. J. Anz, R. L. Whetten, *J. Phys. Chem.* **1991**, *95*, 11–12.
[45] F. Wilkinson, W. P. Helman, A. B. Ross, *J. Phys. Chem. Ref. Data* **1995**, *24*, 663–1021.
[46] R. V. Bensasson, E. Bienvenue, C. Fabre, J. M. Janot, E. J. Land, S. Leach, V. Leboulaire, A. Rassat, S. Roux, P. Seta, *Chem. Eur. J.* **1998**, *4*, 270–278.
[47] R. Stackow, G. Schick, T. Jarrosson, Y. Rubin, C. S. Foote, *J. Phys. Chem. B* **2000**, *104*, 7914–7918.
[48] R. V. Bensasson, M. Schwell, M. Fanti, N. K. Wachter, J. O. Lopez, J.-M. Janot, P. R. Birkett, E. J. Land, S. Leach, P. Seta, R. Taylor, F. Zerbetto, *ChemPhysChem* **2001**, *2,* 109–114.
[49] R. V. Bensasson, E. Bienvenue, J. M. Janot, E. J. Land, S. Leach, P. Seta, *Chem. Phys. Lett.* **1998**, *283*, 221–226.
[50] A. P. Darmanyan, J. W. Arbogast, C. S. Foote, *J. Phys. Chem.* **1991**, *95*, 7308–7312.
[51] R. V. Bensasson, M. N. Berberan-Santos, M. Brettreich, J. Frederiksen, H. Gottinger, A. Hirsch, E. J. Land, S. Leach, D. J. McGarvey, H. Schonberger, C. Schroder, *Phys. Chem. Chem. Phys.* **2001**, *3*, 4679–4683.
[52] Y. Rio, G. Accorsi, H. Nierengarten, J. L. Rehspringer, B. Honerlage, G. Kopitkovas, A. Chugreev, A. Van Dorsselaer, N. Armaroli, J.-F. Nierengarten, *New J. Chem.* **2002**, *26*, 1146–1154.
[53] P. A. Liddell, G. Kodis, J. Andréasson, L. de la Garza, S. Bandyopadhyay, R. H. Mitchell, T. A. Moore, A. L. Moore, D. Gust, *J. Am. Chem. Soc.* **2004**, *126*, 4803–4811.
[54] S. Fratiloiu, L. P. Candeias, F. C. Grozema, J. Wildeman, L. D. A. Siebbeles, *J. Phys. Chem. B* **2004**, *108*, 19967–19975.
[55] P. A. van Hal, R. A. J. Janssen, G. Lanzani, G. Cerullo, M. Zavelani-Rossi, S. De Silvestri, *Phys. Rev. B* **2001**, *64*, 075206.
[56] H. Hoppe, M. Niggemann, C. Winder, J. Kraut, R. Hiesgen, A. Hinsch, D. Meissner, N. S. Sariciftci, *Adv. Funct. Mater.* **2004**, *14*, 1005–1011.
[57] J. N. Demas, G. A. Crosby, *J. Phys. Chem.* **1971**, *75*, 991.
[58] K. Nakamaru, *Bull. Chem. Soc. Jpn.* **1982**, *55*, 2697–2705.
[59] S. R. Meech, D. Phillips, *J. Photochem.* **1983**, *23*, 193–217.
[60] E. Allard, J. Cousseau, J. Ordúna, J. Garin, H. Luo, Y. Araki, O. Ito, *Phys. Chem. Chem. Phys.* **2002**, *4*, 5944–5951.

Received: March 19, 2006
Published online: September 6, 2006

